doi:10.1093/jmcb/mjs048
Published online August 24, 2012

Article

Activation of the ATM-Snail pathway promotes breast cancer metastasis

Mianen Sun[1,†], Xiaojing Guo[1,2,†], Xiaolong Qian[2,†], Haibo Wang[1], Chunying Yang[1], Kathryn L. Brinkman[1], Monica Serrano-Gonzalez[1], Richard S. Jope[3], Binhua Zhou[4], David A. Engler[5], Ming Zhan[6,7], Stephen T.C. Wong[6,7], Li Fu[2,*], and Bo Xu[1,7,*]

[1] Department of Radiation Oncology, The Methodist Hospital Research Institute, Houston, TX 77030, USA
[2] Department of Breast Cancer Pathology and Research Laboratory, Key Laboratory of Breast Cancer of Breast Cancer Prevention and Therapy, Tianjin Medical University Cancer Institute and Hospital, Tianjin 300060, China
[3] Department of Cell Biology, University of Alabama at Birmingham, Birmingham, AL 35294, USA
[4] Department of Biochemistry, University of Kentucky at Lexington, Lexington, KY 40506, USA
[5] The Proteomics Programmatic Core, The Methodist Hospital Research Institute, Houston, TX 77030, USA
[6] Department of Systems Medicine and Bioengineering, The Methodist Hospital Research Institute, Houston, TX 77030, USA
[7] NCI Center for Modeling Cancer Development, Houston, TX 77030, USA
[†] These authors contributed equally to this work.
[*] Correspondence to: Bo Xu, E-mail: boxu2002@yahoo.com; Li Fu, E-mail: fuli@tmu.edu.cn

The DNA damage response (DDR) is critical for the maintenance of genetic stability and serves as an anti-cancer barrier during early tumorigenesis. However, the role of the DDR in tumor progression and metastasis is less known. Here, we demonstrate that the ATM kinase, one of the critical DDR elements, is hyperactive in late stage breast tumor tissues with lymph-node metastasis and this hyperactivity correlates with elevated expression of the epithelial–mesenchymal transition marker, Snail. At the molecular level, we demonstrate that ATM regulates Snail stabilization by phosphorylation on Serine-100. Using mass spectrometry, we identified HSP90 as a critical binding protein of Snail in response to DNA damage. HSP90 binds to and stabilizes phosphorylated Snail. We further provide *in vitro* and *in vivo* evidence that activation of ATM-mediated Snail phosphorylation promotes tumor invasion and metastasis. Finally, we demonstrate that Snail Serine-100 phosphorylation is elevated in breast cancer tissues with lymph-node metastasis, indicating clinical significance of the ATM-Snail pathway. Together, our findings provide strong evidence that the ATM-Snail pathway promotes tumor metastasis, highlighting a previously undescribed role of the DDR in tumor invasion and metastasis.

Keywords: ATM, snail, metastasis

Introduction

Cancer metastasis is the major cause for cancer mortality. Epithelial–mesenchymal transition (EMT) is the initial step for cancer invasion and metastasis. The hallmark of EMT is the loss of the expression of E-cadherin, a cell–cell adhesion protein, which allows cancer cells to gain mobility, leave the primary tumor site, and invade adjacent tissues (Huber et al., 2005). Snail, as a transcription repressor, binds E-boxes of E-cadherin and then inhibits E-cadherin expression. Therefore, Snail is considered essential for triggering EMT during tumor progression (Thiery, 2002) and has been implicated in the acquisition of invasive growth phenotypes of tumors (Nieto, 2002). Snail is over-expressed in a variety of human malignancies, especially in breast cancers (Poser et al., 2001; Blanco et al., 2002; Jiao et al., 2002; Rosivatz et al., 2002). Snail is phosphorylated by glycogen synthase kinase-3β (GSK-3β) on six serine sites (Serines 96, 100, 107, 111, 115, and 119) and these phosphorylation events are required for Snail translocation and degradation (Zhou et al., 2004). Notably, Pak1 (p21 activated kinase-1) is activated by ionizing irradiation (IR) and is responsible for Snail Serine 246 phosphorylation, which functions to maintain Snail nuclear localization and stabilization (Yang et al., 2005; Escriva et al., 2008). Additionally, protein kinase D1 (PKD1) has recently been shown to play an inhibitory role in cancer metastasis by phosphorylation of Snail on Serine 11 (Du et al., 2010).

Optimal DNA damage responses (DDRs) are critical to prevent genetic instability and tumorigenesis (Kastan, 2008). DDR pathways are orchestrated by multiple elements, including sensors, transducers, and effectors. One central protein in the DDR is the ATM kinase (Shiloh, 2001). ATM is mutated in the human autosomal recessive disorder called ataxia telangiectasia (A-T). A-T patients are characterized by progressive neurodegeneration, immunodeficiency, cancer predisposition, and hypersensitivity to IR (Lavin, 2008). In response to DNA damage, ATM is activated and in turn phosphorylates a series of substrates to initiate an optimal DDR (Matsuoka et al., 2007). Recent evidence has suggested that the

Received March 28, 2012. Revised June 30, 2012. Accepted July 20, 2012.

DDR is an oncogene-inducible biological barrier that prevents early stages of tumorigenesis (Bartkova et al., 2005b, 2006; Gorgoulis et al., 2005). The DDR is also critical to promote cellular survival in response to DNA damage as targeting optimal DDR pathways likely leads to radiosensitization (Kastan and Bartek, 2004). Despite the well-characterized roles in cancer initiation and tumor responses to DNA damaging agents, it is less clear whether and how the DDR might play a role in cancer progression and metastasis.

Here, we report a novel mechanism of tumor metastasis involving ATM and its regulation of Snail. We found that ATM is hyperactivated in breast tumor tissues with lymph-node metastasis and that this hyperactivity correlates with elevated expression levels of Snail. We demonstrate that ATM phosphorylates Snail on Serine 100, resulting in resistance to GSK-3β-mediated degradation. Additionally, activation of ATM-mediated Snail phosphorylation in tumors promotes invasion and metastasis. Clinical samples show that Snail Serine 100 phosphorylation is elevated in breast cancer tissues with lymph-node metastasis, highlighting the clinical significance of the ATM-Snail pathway.

Results

Hyperactivation of the ATM kinase correlates with snail over-expression in human breast cancer tissues

Previous studies have demonstrated that constitutive activation of DDR pathways exists in human cancer tissues at different stages, including pre-invasive carcinomas *in situ* (Bartkova et al., 2005a, b; Gorgoulis et al., 2005). However, it was less clear whether DDR hyperactivation was associated with tumor metastasis. To test this possibility, we conducted immunohistochemistry on 296 cases of invasive breast carcinoma tissues. We found that 202 cases (68.2%) were stained positively by the phospho-ATM Serine 1981 antibody (pS1981-ATM) (Figure 1A), a molecular marker of activated ATM (Bakkenist and Kastan, 2003). Interestingly, we found that expression of pS1981-ATM, but not total ATM, positively correlated with the number of lymph-node metastasis cases ($P < 0.001$ and 0.085 for pS1981-ATM and total-ATM, respectively, χ^2 test) (Figure 1B and Supplementary Figure S1A and B). The specificity of the pS1981-ATM antibody was confirmed by immunohistochemistry in the human fibroblast cell line GM9607 (ATM-deficient) into which vector, wild-type (WT), or the serine to alanine (S1981A) mutant ATM was reintroduced (Supplementary Figure S1C). We also measured the expression of Snail, an important EMT marker, in the clinical specimens. We found that 212 cases (71.6%) were positively stained by an anti-Snail antibody (Figure 1C), and that Snail expression highly correlated with lymph-node metastasis ($P < 0.0001$, χ^2 test, Figure 1D). A correlative study showed that there was a significant and positive correlation between hyperactivated ATM and over-expression of Snail ($P < 0.001$, Pearson's correlation test; Figure 1E). These data indicate a

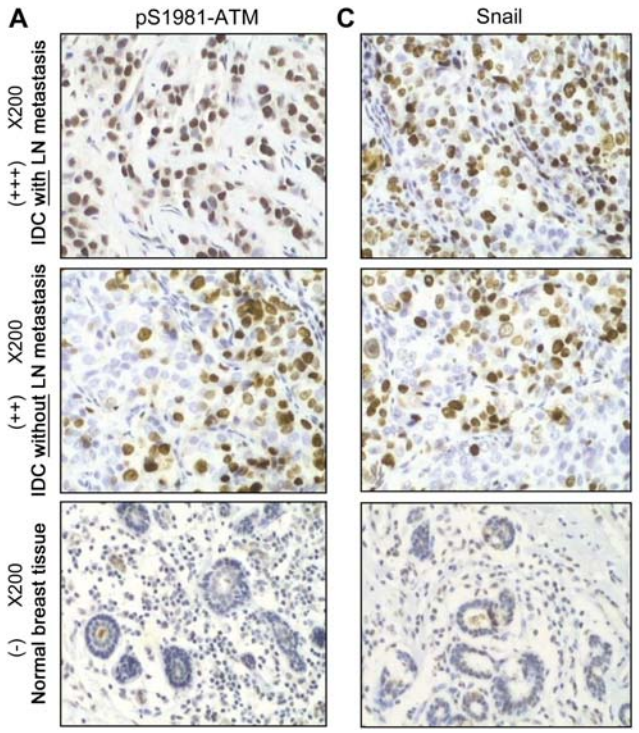

B

pS1981-ATM	Lymph node metastasis		*P*-value
	negative	positive	
-	51	43	
+	24	50	
++	18	44	<0.001*
+++	17	49	

D

Snail	Lymph node metastasis		*P*-value
	negative	positive	
-	50	34	
+	23	38	
++	21	56	<0.0001*
+++	16	58	

E

Snail	pS1981-ATM				*P*-value
	-	+	++	+++	
-	36	11	25	12	
+	17	25	12	7	
++	24	22	17	14	<0.001**
+++	17	16	8	33	

* Chi-Square test; ** Pearson correlation test.

Figure 1 ATM hyperactivation correlates with elevated Snail expression in human invasive breast cancer tissues with lymph-node metastasis. Immunohistochemistry was performed using the pS1981-ATM (**A**) or Snail (**C**) antibody in 296 human breast invasive ductal carcinoma (IDC) tissues. The number of positively stained cases of pS1981-ATM or Snail was shown in (**B**) or (**D**). Note that the different sizes of tumor and normal sizes were demonstrated in Supplementary Figure S1D. The *H*-score method combines the values of the immunereaction intensity and the percentage of tumor cells stained. (−) = no positive cells, (+) = 1%–10% of the cells stained, (++) = 11%–50% of the cells stained, and (+++) = 51%–100% of the cells stained. For **B** and **D**, the χ^2 statistic test was used to assess the correlation. For **E**, the Pearson correlation assay was performed for the correlation analysis.

correlation of ATM activation and Snail expression in breast cancer tissues with lymph-node metastasis. We also conducted a survival analysis. As shown in Supplementary Figure S1E, hyper-activation of ATM (expression of ATM Ser1981p) did not correlate with poor prognosis ($P = 0.264$). Meanwhile, over-expression of Snail showed a significant correlation with poor disease-free survival ($P = 0.047$).

ATM is required for Snail stabilization in response to DNA damage

To investigate a potential regulation of Snail by ATM, we first tested whether ATM activity regulates Snail expression. Because the basal expression level of Snail is fairly low in many cell lines, we utilized camptothecin (CPT), a topoisomerase I poison which was previously shown to up-regulate Snail (Sun et al., 2011), to induce higher expression levels of Snail. As shown in MCF-7 (Figure 2A) or MDA-MB-231 (Figure 2B) cells, CPT-induced Snail up-regulation was abrogated by the inhibition of ATM activity using an ATM-specific inhibitor, Ku55933 (Hickson et al., 2004). To exclude potential off-target effects of Ku55933, we utilized a pair of isogenic HeLa cell lines in which control or ATM shRNA were stably transfected (Yang et al., 2011) and treated them with CPT in the presence or absence of Ku55933. We found that Ku55933 reduced Snail levels in control cells but not in ATM knock-down cells (Supplementary Figure S2A). Interestingly, we also found that basal levels of Snail expression were positively regulated by ATM kinase activity, as Ku55933 could reduce Snail expression in vehicle-treated cells (Figure 2A and B). These observations were confirmed in lymphoblast cell lines with proficient (GM0536) or deficient (GM1526) ATM (Figure 2C) and in the isogenic HeLa cells (Figure 2D). In addition to CPT, we also examined if IR induced Snail up-regulation. We found that the Snail expression level increased at 1 and 2 h after IR, but returned to normal beginning 4 h after IR (Supplementary Figure S2B). Furthermore, we demonstrated that after ATM was knocked down by two different sequences of siRNA against ATM in MDA-MB-231 cells, Snail up-regulation induced by either CPT or IR was abrogated (Supplementary Figure S2C).

We further measured Snail mRNA to clarify if the regulation occurs at the mRNA or protein level. As shown in Figure 2E, CPT treatment increased the Snail mRNA level. Ku55933 did not affect the up-regulation of mRNA, but inhibited Snail at the protein level, indicating that the transcriptional up-regulation of Snail in response to DNA damage is independent of ATM and that ATM-mediated Snail regulation is at the post-transcriptional level. We then tested whether the defect of Snail up-regulation by ATM inhibition could be recovered by blocking proteasome degradation with the proteasome inhibitor MG-132. These results showed that reducing Snail levels by the inhibition of ATM in

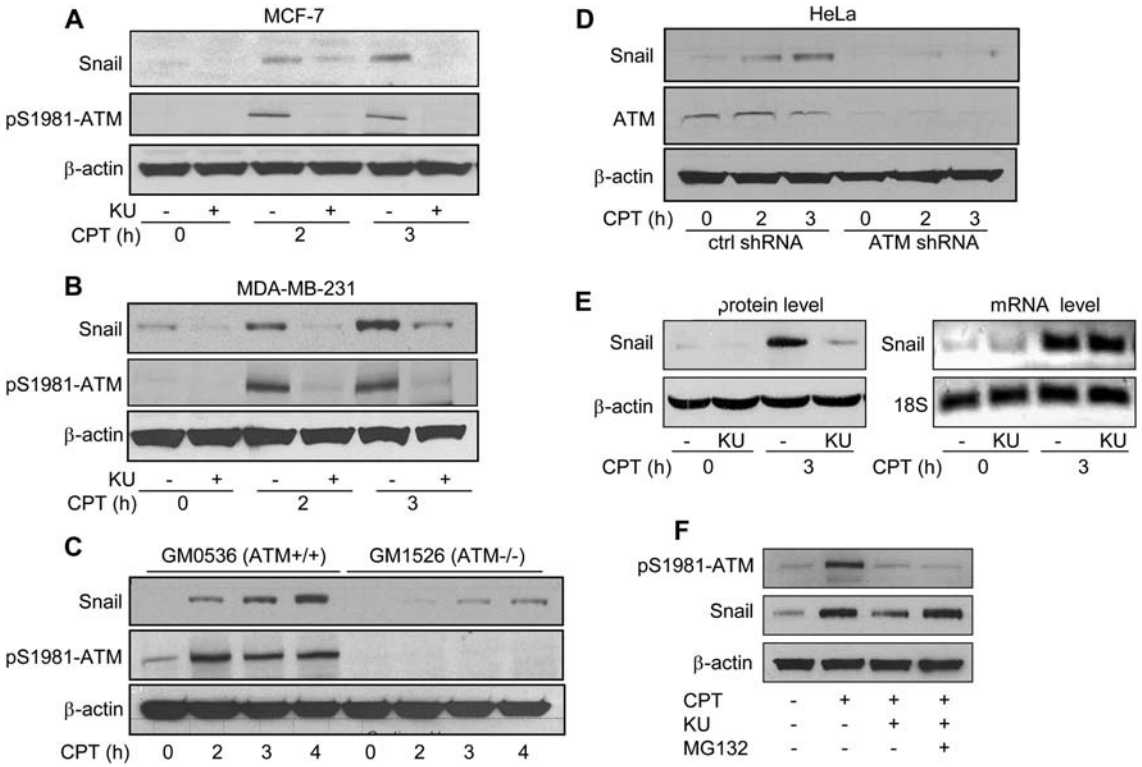

Figure 2 ATM regulates Snail stabilization in response to DNA damage. MCF-7 cells (**A**) or MDA-MB-231 cells (**B**) were pretreated with Ku55933 (10 μM) for 1 h followed by CPT (2 μM) treatment for 2 or 3 h. Total cell lysates were collected and Snail and β-actin were immunoblotted. (**C**) GM0536 and GM1526 cells were treated with CPT (2 μM) for 2, 3, or 4 h, followed by immunoblotting with Snail, pS1981-ATM, and β-actin. (**D**) Snail and ATM levels were detected in control shRNA and ATM shRNA HeLa cells after treatment with CPT for 0, 2, or 3 h. (**E**) MDA-MB-231 cells were pretreated with Ku55933 for 1 h, followed by CPT treatment for 3 h. Snail protein and mRNA levels were measured. β-Actin and 18S were used as loading controls for protein and mRNA, respectively. (**F**) MDA-MB-231 cells were pretreated with MG-132 (10 μM) for 3 h in the presence or absence of Ku55933, followed by CPT treatment for 2 h. Total cell lysates were immunoblotted with indicated antibodies.

response to CPT treatment can be restored in the presence of MG132 (Figure 2F). Taken together, our data demonstrate that ATM positively regulates Snail stabilization in response to DNA damage.

Knockdown of GSK-3β does not affect ATM-mediated Snail stabilization in response to DNA damage

Since GSK-3β is the primary kinase responsible for regulating Snail localization and stabilization (Zhou et al., 2004), we investigated whether ATM regulation of Snail was dependent on GSK-3β. To address this question, we utilized a pair of isogenic GSK-3β knock-down MDA-MB-231 cell lines (Sun et al., 2008). We found that GSK-3β knock-down did not alter the inhibitory effect of Ku55933 on Snail (Supplementary Figure S3), indicating that GSK-3β is dispensable for ATM-mediated Snail stabilization in response to DNA damage.

ATM phosphorylates Snail on Serine 100

Since Snail is a phospho-protein and phosphorylation of Snail regulates its function, we hypothesized that Snail was a direct target of ATM. By investigating the Snail protein sequence, we noticed that there was only one potential ATM phosphorylation site (Serine 100) that matches the ATM consensus motif (S/T-Q) (Kastan and Lim, 2000). Serine 100 is one of the six serine sites that can be phosphorylated by GSK-3β and is well conserved (Figure 3A). To determine if ATM phosphorylates Snail on Serine 100, we first used a commercially available anti-phospho S/T-Q antibody to look for potential phosphorylation by immunoprecipitation of the endogenous Snail. We found that a strong phosphorylation signal was induced by CPT treatment (Figure 3B). To investigate whether the antibody indeed recognized Serine 100 phosphorylation, we generated the flag-tagged WT or the serine to alanine mutant Snail and stably expressed the exogenous proteins in HEK293 cells. We detected Serine 100 phosphorylation only in exogenous WT Snail immunoprecipitates after CPT treatment, and we found that the S100A mutation abrogated the phosphorylation signal (Figure 3C). These data indicate that Snail Serine 100 is phosphorylated in response to CPT treatment. To further study Snail Serine 100 phosphorylation *in vivo*, we developed an anti-phospho-Snail Ser100 antibody which specifically recognizes the phospho-Ser100 site of Snail (Supplementary Figure S4). Using this antibody in isogenic cell lines with control or ATM knock-down, we found that endogenous Snail Serine 100 phosphorylation was inducible in response to DNA damage only when ATM was present (Figure 3D), demonstrating that ATM is required for Snail Serine 100 phosphorylation. DNA damage-induced and ATM-mediated Snail phosphorylation was further demonstrated in MDA-MB-231 and HEK293 cells in response to IR (Figure 3E). To test whether there is direct phosphorylation of Snail Serine 100 by ATM *in vitro*, we utilized an *in vitro* kinase assay (Yang et al., 2012) employing a C-terminal ATM fragment (a.a. 2709–2964), which contains the phosphatidylinositol 3-kinase (PI-3K) domain of the kinase, in the presence of non-phospho-Snail peptides containing the Serine 100 sequence. An N-terminal ATM fragment (a.a. 248–522), which does not possess kinase activity, was used as a negative control for the assay. The anti-phospho-Snail Ser100 antibody was able to detect signals when non-phosphorylated Snail peptides were incubated with C-terminal ATM in the presence of ATP (Figure 3F). These observations indicate that ATM phosphorylates Snail on Serine 100.

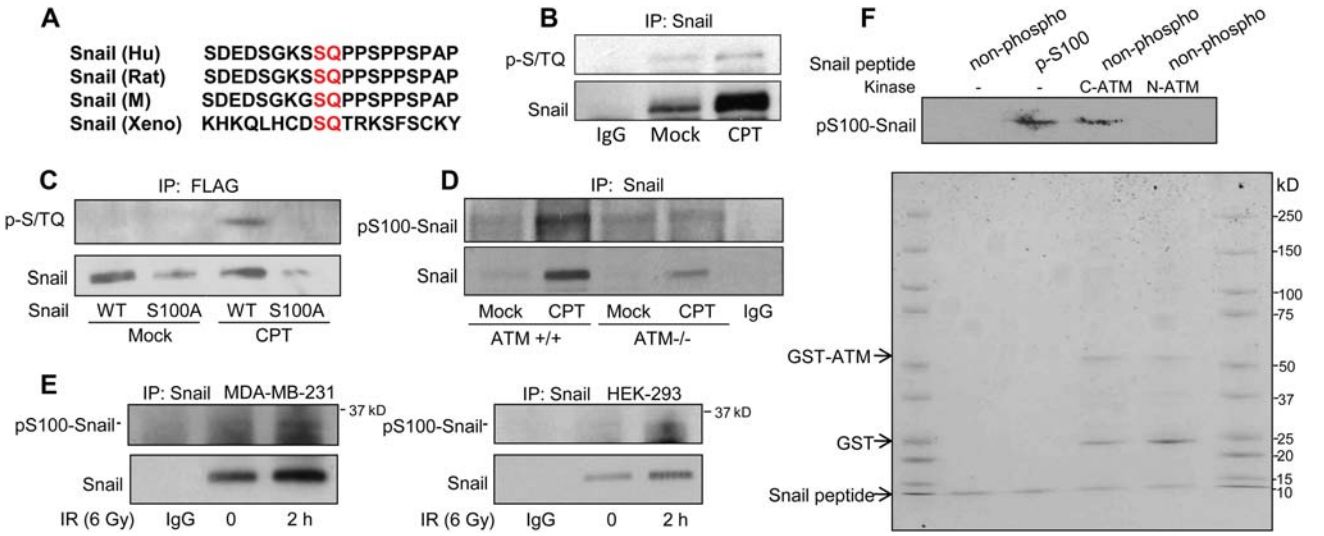

Figure 3 ATM phosphorylates Snail on Serine 100. (**A**) The ATM phosphorylation consensus sequence of Snail in human, rat, mouse, and *Xenopus*. (**B**) Snail was immunoprecipitated from mock- or CPT-treated MDA-MB-231 cells, followed by immunoblotting with indicated antibodies. (**C**) Flag-tagged WT or the serine 100 to alanine mutant form (S100A) of Snail was stably transfected in HEK293 cells. Cells were treated with CPT, and lysates were immunoprecipitated by anti-Flag beads followed by immunoblotting with indicated antibodies. (**D**) Isogenic HeLa cells with proficient or deficient ATM were treated with mock or CPT followed by immunoprecipitating Snail and immunoblotting pS100-Snail. (**E**) MDA-MB-231 cells and HEK293 cells were treated with 6 Gy IR, incubated for 2 h, immunoprecipitated for Snail, and immunoblotted to detect pS100 Snail expression levels. (**F**) The *in vitro* kinase assay was performed using ATM fragments (either GST-tagged N-terminal a.a. 248-522 or C-terminal fragments of ATM a.a. 2709-2964) in the presence of non-phosphorylated Snail peptides. The blot was stained by Coomassie blue and immunoblotted with the anti-phospho-S100 Snail antibody.

ATM-mediated Snail Serine 100 phosphorylation leads to stabilization

We noticed a significantly lower expression level of Snail in the S100A mutant Snail cells (Figure 3C). Since Snail is a protein with fast turn over, we hypothesized that ATM phosphorylation of Snail on Serine 100 might affect the protein's stability. To test this notion, we stably expressed vector only or the WT, S100A, or the S100E (serine 100 to glutamic acid substitution, a phospho-mimicking mutation) form of Snail to test Snail stability. We found that the S100A mutant Snail showed a lower expression level when compared with the WT form. In contrast, the S100E mutant Snail showed a much stronger expression level (Figure 4A). However, the mRNA level of the WT or mutant forms of Snail were similar (Figure 4B), indicating that the changes in protein levels were not due to different mRNA expression but to the stability of the exogenous proteins. Furthermore, we found that while the WT or S100A form of Snail levels increased gradually in response to MG132 in a time-dependent manner, S100E Snail was much more stable than WT or S100A of Snail (Figure 4C and D). Together, our data demonstrate that unlike GSK-3β-mediated Snail phosphorylation, which leads to protein degradation, ATM-mediated Serine 100 phosphorylation leads to Snail stabilization. Conversely, WT or S100A Snail degraded significantly faster than S100E Snail in the presence of the protein synthesis inhibitor cycloheximide (Figure 4E and F).

Since the interaction of Snail and GSK-3β is required for Snail degradation, we further tested whether ATM-mediated Snail phosphorylation reduced the Snail/GSK-3β interaction. To test this hypothesis, we first transfected the vector, flag-tagged WT, S100A, or S100E forms of Snail in HEK293 cells and immunoprecipitated the exogenous proteins. We found that while GSK-3β was pulled down by WT or S100A Snail, it was not detectable in the S100E immunoprecipitates, despite the elevated protein level of S100E (Figure 4G). We then transfected myc-tagged GSK-3β into stable HEK293 cell lines expressing vector, WT, or S100E forms of Snail. Consistent with prior studies (Zhou et al., 2004), over-expression of GSK-3β reduced expression levels of WT Snail. However, the phospho-mimic mutant (S100E) was not down-regulated by GSK-3β (Figure 4H). Taken together, these data strongly demonstrate that ATM-mediated Snail Serine 100 phosphorylation reduces Snail interaction with GSK-3β and inhibits GSK-3β-mediated Snail degradation.

Inhibition of ATM reduces breast cancer cell invasion and migration

Since ATM positively regulates Snail expression, we tested whether ATM inhibitors could reduce tumor cell invasion and metastasis. We utilized the matrigel invasion and wound healing migration assays in cells treated with vehicle or Ku55933. We found that the invasion ability of the highly invasive breast cancer cell line MDA-MB-231 significantly decreased after treatment with

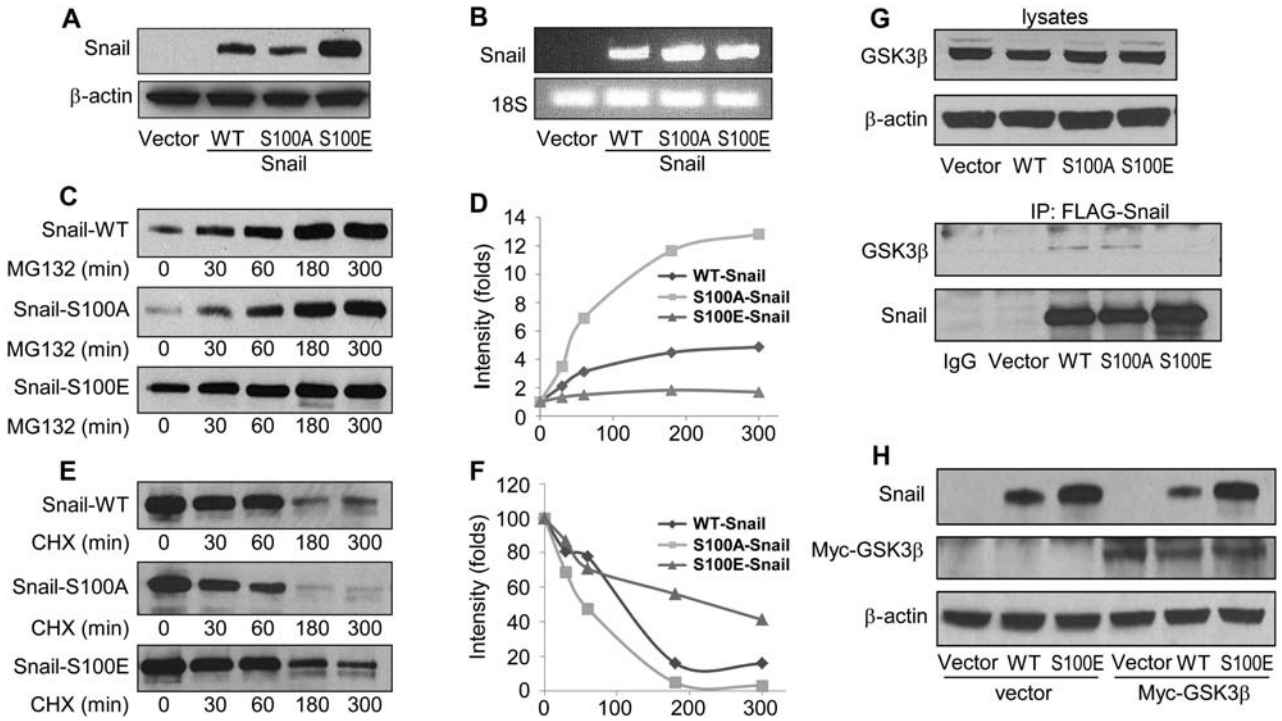

Figure 4 ATM-mediated Snail Serine 100 phosphorylation leads to Snail stabilization. Snail and β-actin protein levels (**A**) and Snail and 18S mRNA levels (**B**) were detected in HEK293 cells stably expressing vector, WT, S100A, or S100E of Snail. (**C**) The stable cell lines were treated with MG-132 (10 μM) for 0, 30, 60, 180, or 300 min, followed by immunoblotting with an anti-Snail antibody. (**D**) The intensity value of Snail expression in **C**. (**E**) HEK293 cells stably expressing WT, S100A, and S100E of Snail were treated with cycloheximide (10 μg/ml) for indicated time points, followed by Snail level measurement (**E**) and quantification (**F**). (**G**) The WT, S100A, or S100E form of Snail in HEK293 cells was immunoprecipitated, and associated GSK-3β levels were measured by immunoblotting (the bottom two panels). Total GSK-3β and β-actin levels are also shown on the top panels. (**H**) Vector, WT-Snail, and S100E-Snail expressing HEK293 cells were transfected with either vector or Myc-GSK-3β. Snail and Myc-GSK-3β levels were determined by immunoblotting.

Ku55933 (Figure 5A). Similarly, measurement of migration using the wound healing assay showed Ku55933 significantly reduced cell migration (Figure 5B and C). These data are consistent with a recent study of an ATM inhibitor Ku60019 on tumor cell invasion and migration (Golding et al., 2009). To further test the role of ATM in invasion and migration, we transiently knocked down ATM by siRNA (Figure 5D) and conducted the matrigel assay in HeLa cells. As shown in Figure 5E, we found that ATM knock-down cells had a significantly reduced invasion index. These data provide strong evidence that the inhibition of ATM reduces invasion and migration. It is noted that Snail knock-down did not affect ATM expression (Figure 5F). Taken together, our data strongly support the conclusion that ATM is a novel target to inhibit breast cancer cell invasion and migration.

ATM-mediated snail phosphorylation increases cancer cell invasion and migration

In order to study the functional significance of ATM-mediated Snail phosphorylation, we transiently expressed vector only, the WT, S100A, or S100E mutant form of Snail in HeLa cells to characterize cellular phenotypes. Since E-cadherin is a target protein repressed by Snail (Thiery, 2002), we tested the effect of Snail Serine 100 mutation on E-cadherin promoter activity using the E-cadherin promoter luciferase assay. We found in HeLa and HEK cells, exogenous WT Snail did not show significant changes on endogenous E-cadherin activity and level, or migration and invasion abilities (Figure 6A). This is consistent with previous results reported by Zhou et al. S100A Snail expression also resulted in a limited effect on EMT induction. However, S100E Snail potently repressed the E-cadherin promoter activity and significantly down-regulated E-cadherin expression (Figure 6B). We also found that the level of vimentin, a type III intermediate filament protein that is expressed in mesenchymal cells (Vuoriluoto et al., 2011), significantly increased after expression of S100E Snail. To further study the functional significance of Serine 100 phosphorylation, we conducted the matrigel invasion assay to examine the invasion ability of cells when Snail Serine 100 is hyperphosphorylated. As shown in Figure 6C, we found that cells expressing S100E Snail showed a significantly higher invasion ability ($P = 0.007$) than those expressing WT or S100A forms of Snail. We also tested whether ATM phosphorylation of Snail affected cell migration using the wound healing assay. We found that S100E Snail expressing cells showed a significantly increased migration rate when compared with WT Snail ($P = 0.0046$) (Figure 6D and E). Taken together, these data demonstrate that ATM phosphorylation of Snail leads to higher invasion and migration abilities.

ATM-mediated snail phosphorylation increases breast cancer metastasis in vivo

To test the functional significance of ATM-mediated Snail phosphorylation *in vivo*, we generated stable MDA-MB-231 cell lines expressing vector, the WT, S100A, or S100E mutant form of Snail. The cells were injected into BALB/c nude mice to generate lung metastases. As shown in Figure 6F and G, we found that cells expressing S100E Snail showed a significantly higher lung metastasis rate ($P = 0.031$) when compared with those expressing WT Snail. However, S100A Snail expression did not show a significant difference with WT Snail. These observations strongly indicate that the functional role of ATM-mediated Snail Serine 100 phosphorylation of Snail is associated with promoting breast cancer metastasis.

HSP90 associates with and stabilizes snail in response to DNA damage

To further investigate the mechanisms of ATM-mediated Snail phosphorylation and its function, we looked for associated proteins that might play a role in ATM phosphorylation of Snail using mass spectrometry. Among the proteins identified, we noticed that there was one associated band that showed a significant increase in expression levels in response to CPT. The mass

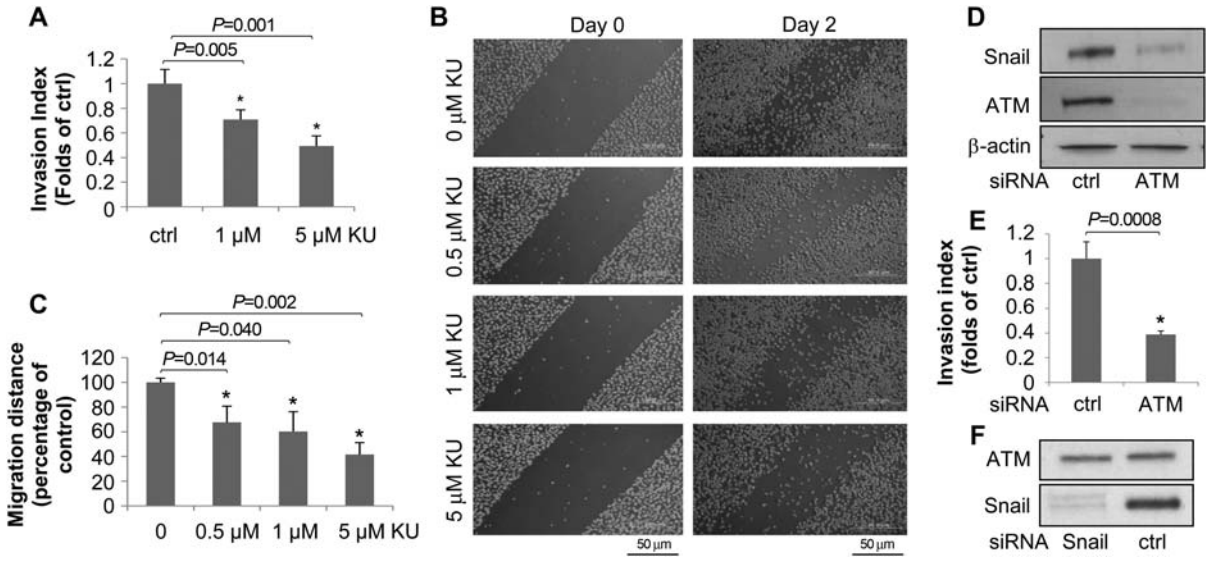

Figure 5 Inhibition of ATM reduces breast cancer cell invasion and metastasis. (**A**) MDA-MB-231 cells were treated with Ku55933 (0, 1, or 5 μM) for 24 h, followed by measurement of the invasion index (mean ± SD). (**B** and **C**) MDA-MB-231 cells were treated with Ku55933 at indicated doses for 0, or 48 h, and pictures (**B**) were taken and migration distances (**C**) were measured and quantified. (**D** and **E**) HeLa cells were transfected with control or ATM siRNA for 48 h, and the Snail level were determined (**D**) and the invasion assay was performed (**E**). (**F**) MDA-MB-231 cells were transfected with control or Snail siRNA followed by immunoblotting with indicated antibodies.

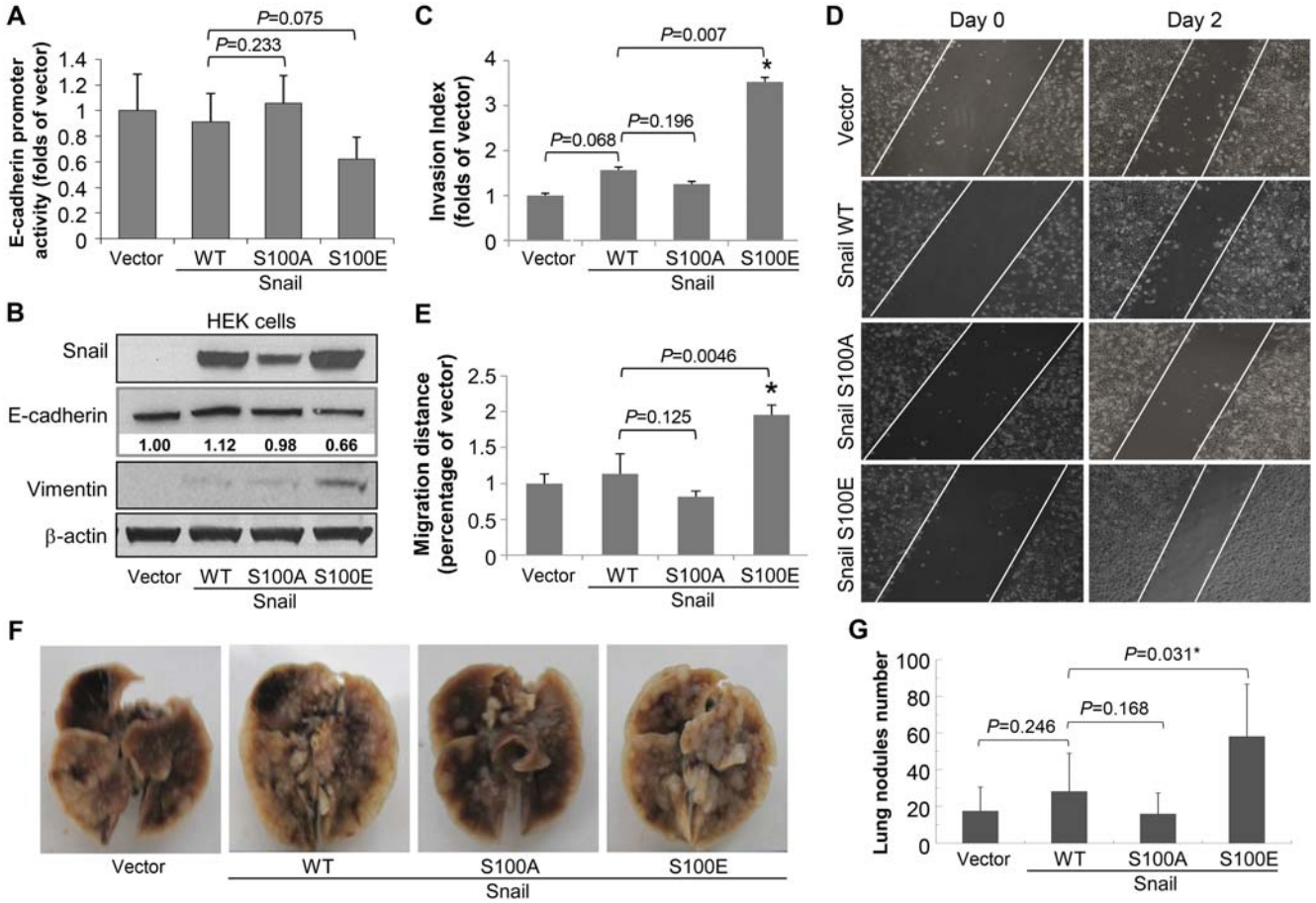

Figure 6 ATM phosphorylation of Snail promotes tumor invasion and metastasis. (**A**) HeLa cells were co-transfected with vector, WT, S100A, or S100E mutant forms of Snail with the E-cadherin promoter plasmid. Forty-eight hours after transfection, cells were lysed, and the luciferase activity was determined. (**B**) HEK293 cells were transfected with vector, WT, S100A, or S100E. Thirty-six hours after transfection, total cell lysates were collected followed by immunoblotting with indicated antibodies. (**C**) The matrigel invasion assay was performed after HeLa cells were transiently transfected with vector, WT, or S100A or S100E of Snail. Shown are mean ± SD, $n = 3$. (**D**) HeLa cells were transiently transfected with vector, WT, S100A, or S100E of Snail. Twenty-four hours after transfection, the wound healing assay was conducted. Photos were taken at 24 (Day 0) and 72 h (Day 2) after transfection. (**E**) Results in **D** were quantified. Shown are mean ± SD, $n = 3$, $^*P \leq 0.05$. (**F** and **G**) Isogenic MDA-MB-231 cells expressing vector, WT, S100A, or S100E of Snail were injected via the tail vein of BALB/c nude mice. Eight weeks after injection, the mice were sacrificed and lungs were removed. Lung metastasis was measured by counting metastatic nodules in the lungs. Representative photographs of the lung are shown in **F** and the number of lung metastases nodules were plotted (mean ± SD, $n = 8$, $^*P \leq 0.05$) (**G**).

spectrometry analysis identified the protein as HSP90 α and β (Supplementary Figure S5). To validate the mass spectrometry result, we conducted co-immunoprecipitation experiments in cells treated with vehicle or CPT. We found that HSP90 associated with Snail in response to CPT (Figure 7A). To study whether HSP90 interaction with Snail was dependent on Snail phosphorylation, we utilized stable HEK293 cell lines expressing WT or the S100A mutant form of Snail. We found that while WT-Snail associated with HSP90α in response to CPT, the S100A mutation abrogated the interaction (Figure 7B). In another set of experiments with transient expression of WT, S100A, or S100E, we found that HSP90α was associated with S100E Snail with a much stronger affinity than with either WT or S100A (Figure 7C). These data indicate that ATM-mediated Serine 100 phosphorylation is critical for the HSP90α–Snail association. Since HSP90 is a chaperone protein which regulates the stability of client proteins (Taipale et al., 2010), we hypothesized that HSP90α is required for Snail stabilization. To test this notion, we expressed WT or S100E Snail in isogenic 293T cell lines expressing control shRNA or shRNA-HSP90α (Barksdale and Bijur, 2009). We found that in HSP90α knock-down cells, S100E showed significantly reduced stabilization of Snail, compared with S100E in cells with proficient HSP90α (Figure 7D). We also utilized an HSP90 inhibitor, 17-(dimethylaminoethylamino)-17-demethoxygeldanamycin (17-DMAG), to examine if the activity of HSP90 affects Snail stability. We found that 17-DMAG significantly reduced Snail stabilization in response to CPT or IR (Figure 7E). Together, our data demonstrate that HSP90α associates with the Ser100 phosphorylated form of Snail to stabilize Snail, indicating that HSP90α is a critical component of the ATM-Snail pathway.

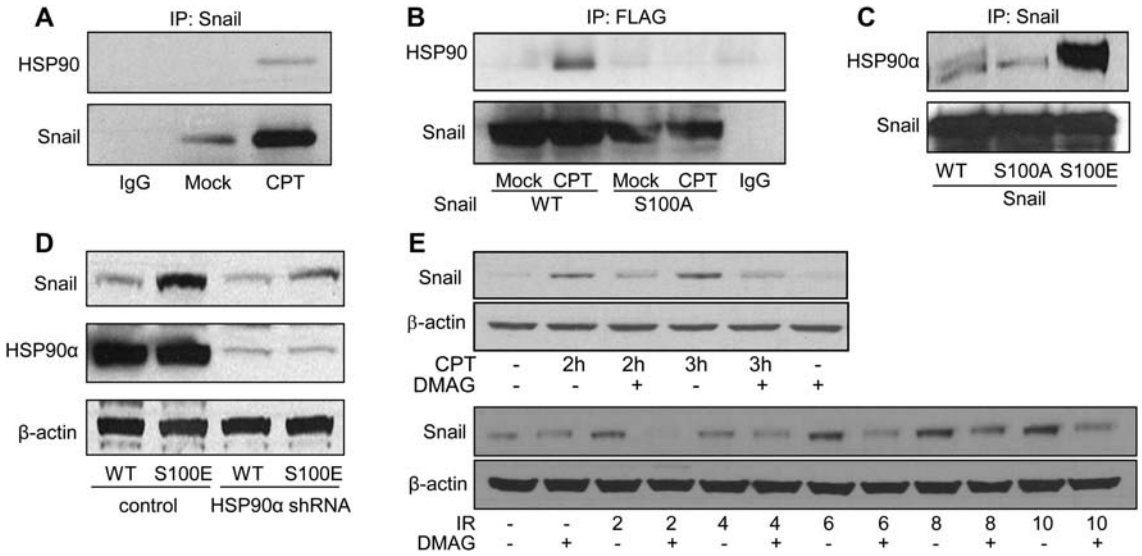

Figure 7 HSP90 interacts with Snail and facilitates Snail stabilization. (**A**) MDA-MB-231 cells treated with mock or CPT were subjected to immunoprecipitation using an anti-Snail antibody. The immunoprecipitates were blotted with indicated antibodies. (**B**) HEK 293 cells expressing WT or S100A of Snail were treated with mock or CPT. Three hours after treatment, cell lysates were immunoprecipitated by the anti-FLAG antibody, followed by immunoblotting with indicated antibodies. (**C**) HeLa cells were transfected with WT, S100A, or S100E Snail. Snail was immunoprecipitated followed by immunoblotting with the indicated antibodies. (**D**) Isogenic cell lines with control or HSP90α knock-down were transfected with WT or S100E of Snail. Thirty-six hours after transfection, cell lysates were harvested and subjected to immunoblotting using the indicated antibodies. (**E**) MDA-MB-231 cells were pretreated with 17-DMAG (0.5 μM) for 24 h in serum-free media followed by CPT or IR treatment for 2 h, and cell lysates were immunoblotted for Snail and β-actin.

Snail Serine 100 phosphorylation is elevated in breast cancer tissues with lymph-node metastasis

To further study the clinical significance of ATM-mediated Snail Serine 100 phosphorylation, we employed additional breast cancer tissues obtained at the Tianjin Medical University Cancer Hospital. Preliminary experiments examining the specificity excluded the use of the pS100-Snail antibody for immunohistochemistry. Therefore, we decided to conduct western blot using extracted proteins from the tumor tissues (Supplementary Figure S6). We quantified the immunoblot signals using Image J. In the total of 80 breast cancer tissues, we found that the correlation of pS100-Snail with lymph-node metastasis is significant ($P \leq 0.001$, *t*-test) (Table 1). Similar results were found for pS1981-ATM and total Snail ($P \leq 0.001$ and $= 0.002$, *t*-test, respectively). To evaluate the correlation of pS100-Snail and pS1981-ATM, we established a standard for the Image J readout as the reading $\geq$ the average reading as a positive signal. Using the Pearson correlation test, we found that pS100-Snail strongly correlated with the expression of pS1981-ATM ($P \leq 0.001$) (Table 2). Collectively, these observations strongly support the clinical significance of ATM-mediated Snail Serine 100 phosphorylation.

Table 1 Correlation of lymph-node metastasis and expression of snail, pS100-Snail, and pS1981-ATM in breast cancer tissues.

	Lymph-node metastasis[a]		*P*-value**
	Negative	Positive	
Snail	0.4653 ± 0.2276	0.6343 ± 0.2145	0.002
pS100-Snail	0.5749 ± 0.2568	0.9276 ± 0.2884	<0.001
pS1981-ATM	0.4031 ± 0.3086	1.0385 ± 0.4419	<0.001

[a]Mean Image-J Readings ± SD, normalized by β-actin. **Student's *t*-test.

Table 2 Correlation of pS100-Snail and pS1981-ATM in breast cancer tissues.

	pS1981-ATM[a]		*P*-value**
	−	+	
pS100-Snail			
−	36	10	<0.001
+	12	22	

[a]'−' means values of Image-J reading <average of the group; '+' means values of Image-J Reading ≥ average of the group. **Pearson's correlation test.

Discussion

The optimal DDR is critical for the maintenance of genome stability and has been shown to be an anti-cancer barrier to prevent early tumorigenesis (Jackson and Bartek, 2009). In the present study, we demonstrate that the ATM kinase, one of the critical DDR components, is hyperactive in breast cancer tissues with lymph-node metastasis. We further demonstrate the correlation of hyperactive ATM and the EMT marker, Snail. At the molecular level, ATM regulates Snail through the phosphorylation of Serine 100. HSP90, a chaperone protein, binds to this phosphorylated form of Snail. Both *in vitro* and *in vivo* evidence show that the activation of the ATM-Snail pathway can increase tumor invasion and metastasis. The clinical significance of ATM-mediated Snail Serine 100 phosphorylation is demonstrated by strong correlation of Serine 100 phosphorylation with lymph-node metastasis in breast cancer tissues. These findings provide a

new understanding of tumor metastasis and highlight dual functions of DDR signaling in tumor initiation and progression.

Recently, NBS1, a component of the DDR Mre11-Rad50-NBS1 complex (Usui et al., 2001), has been reported to be over-expressed in advanced head and neck squamous cell carcinoma (HNSCC), and this over-expression correlated with patient prognosis (Yang et al., 2007). More interestingly, both *in vitro* and *in vivo* evidence revealed that over-expressing NBS1 up-regulated Snail and its downstream target, matrix metalloproteinase-2, in HNSCC. These studies further support our notion that DDR components play a critical role in promoting cancer invasion and metastasis. However, it is noted that the majority of the data for mechanistic studies in our study were obtained from cell lines with transient activation of ATM by CPT and IR treatment. This is in contrast to the *in vivo* situation, in which ATM is constantly activated at a modest level (Figure 1). Further experimental models are needed to confirm the physiological/pathological significance of hyperactive DDR in tumor progression.

The function of Snail in metastasis is regulated by phosphorylation. In some cases, the phosphorylation of Snail by GSK-3β (Zhou et al., 2004; Yook et al., 2005) and PKD leads to Snail degradation (Du et al., 2010). In other cases, Pak1-mediated phosphorylation enhances Snail nuclear localization and transcription activity (Yang et al., 2005), and Casein Kinase-2 and cAMP-activated protein kinase A (PKA)-mediated phosphorylation enhances stability and positively regulates Snail's repressive function (MacPherson et al., 2010). The ATM phosphorylation sequence of Snail falls within the GSK-3β phosphorylation cluster, although the function is distinct. GSK-3β-mediated Snail phosphorylation regulates Snail subcellular localization and ubiquitination. In contrast, ATM-mediated Snail phosphorylation promotes stability. It is less clear how the functional significance of ATM-mediated Ser100 phosphorylation (for stabilization) differs from GSK-3β-mediated phosphorylation (for degradation). In our model, ATM-mediated Serine 100 phosphorylation, which occurs as a result of hyperactive DDR, might cause a conformational change of Snail, increasing the binding affinity with HSP90. This interaction might result in further conformational changes of Snail, leading to reduced GSK-3β/Snail association. The HSP90 and Snail interaction might also competitively inhibit Snail binding with GSK-3β, resulting in resistance to GSK-3β-mediated phosphorylation and degradation. The role of HSP90 in the stabilization of Snail is consistent with recent findings that HSP90 inhibitors are active in reducing tumor metastasis (Tsutsumi et al., 2009).

It is noted that the Snail S100E level slightly increased in HSP90α knockdown cells. Since HSP90α knockdown cells still have HSP90β, it is possible that the partial increase on S100E in the knockdown cells resulted from HSP90β. However, our data demonstrate that HSP90α play a predominant role in the regulation of Snail stability.

ATM-mediated Snail phosphorylation and stabilization might not only affect E-cadherin, since in cells with very low E-cadherin levels, the S100E mutant form of Snail can still increase invasion and migration (Figure 5). Interestingly, we found that vimentin is significantly up-regulated by S100E mutation, indicating that vimentin might be another major target of hyperphosphorylated Snail.

The crosstalk between GSK-3β- and ATM-mediated Snail phosphorylation is also indicated in our studies. For example, the S100E mutant Snail is resistant to GSK-3β-mediated degradation. Since nuclei GSK-3β is activated by DNA damage and the outcome of activated GSK-3β is expected to result in Snail degradation, the up-regulation of Snail in response to DNA damage represents a shift from a negative regulation by GSK-3β to a positive regulation by ATM. Since we observed that the expression level of Snail returns to normal 4 h after IR and ATM activation is still measureable at 4 h, it indicates that a balance is achieved within 4 h after IR and GSK-3β resumes to be a dominant player of the crosstalk.

The physiological stimulus of DNA damage at later stages of tumorigenesis that could activate ATM and promote invasion and metastasis is still not known. It is possible the tumor microenvironment might play a significant role in ATM activation. For example, chronic hypoxic conditions might activate ATM (Hammond and Giaccia, 2004). It is expected the activation of the ATM-Snail pathway is to promote survival, and gaining invasiveness and metastasis becomes an adaptive response of surviving cells.

In addition to Snail, other metastasis regulators are likely to be components of DDR pathways, e.g. transcription repressors of E-cadherin including the Snail/Slug family, Twist, ZEB1, Smad interacting protein 1 (SIP1), and E12/E47 (Peinado et al., 2007). Indeed, PKB/AKT can phosphorylate Twist-1 on Serine 42 to inhibit p53 activity in response to DNA damage (Vichalkovski et al., 2010). ZEB2/SIP1 has an anti-apoptotic activity which is independent of either cell cycle checkpoints or loss of cell–cell adhesion, but associated with reduced phosphorylation of ATM/ATR targets in UV-treated cells (Sayan et al., 2009). The prognostic value of SIP1 and its role in the DDR has indicated a link between genetic instability and metastasis, further supporting our concept of the DDR in promoting tumor invasion and metastasis.

In summary, our data have provided clinical evidence and molecular mechanisms both *in vitro* and *in vivo* to establish a critical link between ATM and Snail and the role of this link in promoting breast tumor invasion and metastasis.

Materials and methods

Cell culture and materials

HeLa, MCF-7, HEK293, and MDA-MB-231 cells (obtained from ATCC) were grown in Dulbecco's modified Eagle's medium (DMEM). GM0536, GM1526, GM0637, and GM9607 cells (obtained from NIGMS Human Mutant Cell Repository) were grown in RPMI 1640 (Hyclone) supplemented with 10% fetal bovine serum (Invitrogen), 100 U/ml penicillin, and 100 μg/ml streptomycin (Cellgro) in humidified 37°C chambers with 5% CO_2. The HSP90 knock-down cells were provided by Dr Gautam N. Bijur. The following sources provided antibodies: Snail, GSK-3β, ATM, phospho-Serine-1981-ATM (Cell Signaling Technology) for immunoblotting. Snail, ATM, phospho-Serine-1981-ATM (Abcam) for immunohistochemistry. HSP90 and E-cadherin (BD Pharmingen), β-actin, and FLAG-tagged antibody (Sigma) for immunoblotting. The phospho-Ser100-Snail antibody was generated by EZBiolab. All horseradish peroxidase-conjugated secondary

antibodies were purchased from Southern Biotechnology Associates. Ku55933 and CPT were purchased from Calbiochem, and 17-(dimethylaminoethylamino)-17-demethoxygeldanamycin (17-DMAG) was purchased from Invivogen. Ionizing radiation was delivered by X-Rad 320 (Precision X-Ray Inc.).

Human breast cancer tissue samples

The initial 296 cases of invasive breast carcinomas, diagnosed in 2003, as well as the additional 80 cases of breast cancer tissues, diagnosed between 2011 and 2012, were obtained from the Department of Breast Pathology and Research Laboratory, Cancer Hospital of Tianjin Medical University, Tianjin, China, with the approval of the Tianjin Medical University IRB committee. All cases were female; 29–75 years of age (mean age 51.8 years).

Immunohistochemistry

Immunohistochemistry using the avidin–biotin–immunoperoxidase technique was performed for Snail, ATM, and pS1981-ATM in the 296 cases of clinical samples. Sections of formalin-fixed tissues from all cases were performed using a standard protocol. Briefly, 4 μm tissue sections on coated slides were heated for antigen retrieval, pretreated with a 3% solution of hydrogen peroxide for 5–10 min, rinsed, and incubated with 10% normal goat serum as a blocking agent. The sections were then incubated sequentially with the primary antibody (pS1981-ATM in a 1:100 dilution, Snail in a 1:100 dilution or ATM in a 1:200 dilution), a biotinylated secondary antibody and avidin–peroxidase conjugate. All steps were preceded by rinsing of sections with PBS (pH 7.6). The chromogen was 3,3′-diaminobenzidine (DAB). The immunoreaction for pS1981-ATM, Snail, and ATM in the nucleus of tumor cells was evaluated independently by two experienced pathologists and scored by the H-score method that combines the values of immunoreaction intensity and the percentage of tumor cell stained as described (Manni et al., 2001; Xia et al., 2004), (−) = no positive cells, (+) = 1%–10% of the cells stained, (++) = 11%–50% of the cells stained, and (+++) = 51%–100% of the cells stained. To test the specificity of the anti-pS1981-ATM antibody, the human fibroblast cell line GM9607 was transfected with vector, the WT, or S1981A form of ATM (provided by Dr Michael B. Kastan) on the Thermo scientific nunc lab-tek II sterile chamber slide system (Fisher scientific) followed by immunohistochemistry in the cultured cells.

Immunoblotting

After washing with PBS twice, cells were harvested or human breast tissues were homogenized in lysis buffer (20 mM Tris, pH 7.5, 50 mM NaCl, 2 mM EDTA, 1 mM sodium orthovanadate, 100 mM phenylmethylsulfonyl fluoride, 10 mg/ml leupeptin, 10 mg/ml aprotinin, 5 mg/ml pepstatin, 50 mM NaF, 1 nM okadaic acid, 1% Triton X-100, and 10% glycerol), centrifuged at 20800 *g* for 10 min, and supernatants were collected. Protein concentrations were determined using the Bradford method (Bio-Rad). Cell lysates were mixed with Laemmli sample buffer and placed in a boiling water bath for 5 min. Proteins were resolved in SDS–polyacrylamide gels and transferred to nitrocellulose. Blots were probed with the indicated primary antibodies, and immunoblots were developed using horseradish peroxidase-conjugated goat anti-mouse or goat anti-rabbit IgG, followed by detection with enhanced chemiluminescence.

Immunoprecipitation

Whole cell lysates were incubated with anti-FLAG or anti-Snail antibodies overnight, and then incubated with protein G for 2 h at 4°C. The samples were then washed three times with 400 ml lysis buffer, suspended in 40 μl Laemmli buffer, placed in a boiling water bath for 5 min, and the proteins resolved by electrophoresis.

In vitro kinase assay

GST-ATM-N (N-terminal, a.a. 248–522) and GST-ATM-C (C-terminal, a.a. 2709–2964) purified from *Escherichia coli* were incubated with un-phosphorylated Snail peptides in the kinase buffer (25 mM Tris–HCl, pH 7.5, 5 mM β-glycerophosphate, 2 mM dithiothreitol, 0.1 mM Na_3VO_4, 10 mM $MgCl_2$, 10 mM Mn_2Cl_2) with 5 mM ATP for 1 h at 30°C. The samples were boiled and fractionated on SDS–PAGE and subjected to Coomassie Blue staining and western blot analysis using the anti-phospho-Serine 100 Snail antibody.

Plasmids and siRNAs

Flag-tagged Snail S100A, S100E constructs were generated by Cellomics Technology, and the sequences of resulting mutant Snail constructs were verified by direct sequencing using the Seq Wright DNA Technology Service. Snail siRNA and ATM shRNA plasmids were purchased from Santa Cruz Biotechnology. The ATM siRNA sequences used in Figure 7D and E are: Sense: 5′-GGCCCUUAAGUUAUUUGAAGAUAaa-3′; antisense: 5′-UUUAUCUUCAAAUAACUUAAGGGCCUU-3′.

E-cadherin promoter luciferase assay

HeLa cells (70% confluent) were transiently transfected with E-cadherin promoter luciferase constructs together with WT or mutant Snail constructs using FuGENE HD reagent (Roche). After 48 h, luciferase activity was measured using a luciferase reporter assay kit according to the manufacturer's instructions (Promega).

Wound healing migration assay

Confluent monolayers of MDA-MB-231 or transfected HeLa cells with or without treatment were 'wounded' using the narrow end of a pipette tip. The wounds were photographed daily (0–2 days) in the same area. Wound healing was measured and recorded for analysis.

Matrigel invasion assay

The FluoroBlok 24-multiwell invasion assay was purchased and used according to the manufacturer's instructions (8 μm pore size; BD Biosciences). Briefly, treated or mock MDA-MB-231 or HeLa cells were collected using trypsin (Invitrogen), and 2.5×10^4 cells were seeded in the upper chambers in serum-free media with mock or treatment. Serum-containing (10% FBS) medium with mock or treatment was added to the lower chambers and the plate was incubated at 37°C with 5% CO_2. After 24 h, the cells were stained with calcein AM for 1 h at 37°C and then fluorescence was measured. The data were collected, analyzed, and statistics conducted.

MTT assay

Cells (3×10^3) in 100 μl culture media were plated in each well of 96-well plate. After overnight incubation, 20 μl of a premixed optimized Dye Solution (Promega) was added to each well. After 2 h incubation at 37°C, absorbance at 570 nm was recorded for analysis.

In vivo lung metastasis model

Female BALB/c nude mice (6–8 weeks old) were purchased from Vital River and maintained under specific pathogen-free conditions. The general health status of the animals was monitored daily. All procedures involving animals and their care were conducted in conformity with the institutional guidelines that are in compliance with national and international laws and policies. Isogenic MDA-MB-231 cell lines stably expressing vector-only, the WT, S100A, or S100E mutant form of Snail were injected into the mice (eight for each group) via the tail vein at a concentration of 2×10^6 cells/mouse. Eight weeks after, mice were sacrificed and lungs were removed and weighed. The lung metastatic nodules were examined macroscopically and detected in paraffin-embedded sections stained with hematoxylin and eosin.

Statistics

Data were analyzed by Student's *t*-test, χ^2 test, or Pearson correlation test; and $P \leq 0.05$ was considered significant.

Survival analysis

For survival analysis, we defined recurrence as any first recurrence at a distant site. Patients were censored from the date of the last follow-up visit for death from causes other than breast cancer, local or regional recurrences, or the development of a second, primary cancer, including contralateral breast cancer. If a patient's status during follow-up indicated a confirmed metastasis without a recurrence date, the follow-up visit date was used. The time to first recurrence, and survival time were calculated relative to the primary diagnosis date. The Kaplan–Meier survival curves were constructed, and between-group differences were tested using the log-rank test.

Human subject and animal study declaration

All human tumor tissues were obtained with written informed consent from patients or their guardians at Tianjin Medical University Cancer Hospital prior to participation in the study. The Institutional Review Board and Institutional Animal Care and Use Committee of the Tianjin Medical University Cancer Institute and Hospital approved the use of the tumor specimens and animal models in this study.

Supplementary material

Supplementary material is available at *Journal of Molecular Cell Biology* online.

Acknowledgements

We gratefully acknowledge Dr Michael B. Kastan (Duke University) and Dr Gautam N. Bijur (The University of Alabama at Birmingham) for providing reagents. We thank all members of the Xu laboratory for help. The mass spectrometry was conducted at the Proteomics Programmatic Core of TMHRI.

Funding

This work was supported by NIH grants R01CA133093, R01ES016354, R21NS061748 and Oshman Foundation to B.X., U54CA149169 to S.W., R01CA125454 to B.Z., and National Natural Science Foundation of China (grant no. 30930038), Program for Changjiang Scholars and Innovative Research Team (grant no. IRT0743), and the National 973 Program of China (grant no. 2009CB521700) to L.F.

Conflict of interest: none declared.

References

Bakkenist, C.J., and Kastan, M.B. (2003). DNA damage activates ATM through intermolecular autophosphorylation and dimer dissociation. Nature *421*, 499–506.

Barksdale, K.A., and Bijur, G.N. (2009). The basal flux of Akt in the mitochondria is mediated by heat shock protein 90. J. Neurochem. *108*, 1289–1299.

Bartkova, J., Bakkenist, C.J., Rajpert-De Meyts, E., et al. (2005a). ATM activation in normal human tissues and testicular cancer. Cell Cycle *4*, 838–845.

Bartkova, J., Horejsi, Z., Koed, K., et al. (2005b). DNA damage response as a candidate anti-cancer barrier in early human tumorigenesis. Nature *434*, 864–870.

Bartkova, J., Rezaei, N., Liontos, M., et al. (2006). Oncogene-induced senescence is part of the tumorigenesis barrier imposed by DNA damage checkpoints. Nature *444*, 633–637.

Blanco, M.J., Moreno-Bueno, G., Sarrio, D., et al. (2002). Correlation of Snail expression with histological grade and lymph node status in breast carcinomas. Oncogene *21*, 3241–3246.

Du, C., Zhang, C., Hassan, S., et al. (2010). Protein kinase D1 suppresses epithelial-to-mesenchymal transition through phosphorylation of snail. Cancer Res. *70*, 7810–7819.

Escriva, M., Peiro, S., Herranz, N., et al. (2008). Repression of PTEN phosphatase by Snail1 transcriptional factor during gamma radiation-induced apoptosis. Mol. Cell. Biol. *28*, 1528–1540.

Golding, S.E., Rosenberg, E., Valerie, N., et al. (2009). Improved ATM kinase inhibitor KU-60019 radiosensitizes glioma cells, compromises insulin, AKT and ERK prosurvival signaling, and inhibits migration and invasion. Mol. Cancer Ther. *8*, 2894–2902.

Gorgoulis, V.G., Vassiliou, L.V., Karakaidos, P., et al. (2005). Activation of the DNA damage checkpoint and genomic instability in human precancerous lesions. Nature *434*, 907–913.

Hammond, E.M., and Giaccia, A.J. (2004). The role of ATM and ATR in the cellular response to hypoxia and re-oxygenation. DNA Repair (Amst.) *3*, 1117–1122.

Hickson, I., Zhao, Y., Richardson, C.J., et al. (2004). Identification and characterization of a novel and specific inhibitor of the ataxia-telangiectasia mutated kinase ATM. Cancer Res. *64*, 9152–9159.

Huber, M.A., Kraut, N., and Beug, H. (2005). Molecular requirements for epithelial–mesenchymal transition during tumor progression. Curr. Opin. Cell Biol. *17*, 548–558.

Jackson, S.P., and Bartek, J. (2009). The DNA-damage response in human biology and disease. Nature *461*, 1071–1078.

Jiao, W., Miyazaki, K., and Kitajima, Y. (2002). Inverse correlation between E-cadherin and Snail expression in hepatocellular carcinoma cell lines in vitro and in vivo. Br. J. Cancer *86*, 98–101.

Kastan, M.B. (2008). DNA damage responses: mechanisms and roles in human disease: 2007 G.H.A. Clowes Memorial Award Lecture. Mol. Cancer Res. *6*, 517–524.

Kastan, M.B., and Bartek, J. (2004). Cell-cycle checkpoints and cancer. Nature *432*, 316–323.

Kastan, M.B., and Lim, D.S. (2000). The many substrates and functions of ATM. Nat. Rev. Mol. Cell Biol. *1*, 179–186.

Lavin, M.F. (2008). Ataxia-telangiectasia: from a rare disorder to a paradigm for cell signalling and cancer. Nat. Rev. Mol. Cell Biol. *9*, 759–769.

MacPherson, M.R., Molina, P., Souchelnytskyi, S., et al. (2010). Phosphorylation of serine 11 and serine 92 as new positive regulators of human Snail1 function: potential involvement of casein kinase-2 and the cAMP-activated kinase protein kinase A. Mol. Biol. Cell *21*, 244–253.

Manni, A., Astrow, S.H., Gammon, S., et al. (2001). Immunohistochemical detection of ornithine-decarboxylase in primary and metastatic human breast cancer specimens. Breast Cancer Res. Treat. *67*, 147–156.

Matsuoka, S., Ballif, B.A., Smogorzewska, A., et al. (2007). ATM and ATR substrate analysis reveals extensive protein networks responsive to DNA damage. Science *316*, 1160–1166.

Nieto, M.A. (2002). The snail superfamily of zinc-finger transcription factors. Nat. Rev. Mol. Cell Biol. *3*, 155–166.

Peinado, H., Olmeda, D., and Cano, A. (2007). Snail, Zeb and bHLH factors in tumour progression: an alliance against the epithelial phenotype? Nat. Rev. Cancer *7*, 415–428.

Poser, I., Dominguez, D., de Herreros, A.G., et al. (2001). Loss of E-cadherin expression in melanoma cells involves up-regulation of the transcriptional repressor Snail. J. Biol. Chem. *276*, 24661–24666.

Rosivatz, E., Becker, I., Specht, K., et al. (2002). Differential expression of the epithelial–mesenchymal transition regulators snail, SIP1, and twist in gastric cancer. Am. J. Pathol. *161*, 1881–1891.

Sayan, A.E., Griffiths, T.R., Pal, R., et al. (2009). SIP1 protein protects cells from DNA damage-induced apoptosis and has independent prognostic value in bladder cancer. Proc. Natl Acad. Sci. USA *106*, 14884–14889.

Shiloh, Y. (2001). ATM and ATR: networking cellular responses to DNA damage. Curr. Opin. Genet. Dev. *11*, 71–77.

Sun, M., Song, L., Li, Y., et al. (2008). Identification of an antiapoptotic protein complex at death receptors. Cell Death Differ. *15*, 1887–1900.

Sun, M., Song, L., Zhou, T., et al. (2011). The role of DDX3 in regulating Snail. Biochim. Biophys. Acta *1813*, 438–447.

Taipale, M., Jarosz, D.F., and Lindquist, S. (2010). HSP90 at the hub of protein homeostasis: emerging mechanistic insights. Nat. Rev. Mol. Cell Biol. *11*, 515–528.

Thiery, J.P. (2002). Epithelial–mesenchymal transitions in tumour progression. Nat. Rev. Cancer *2*, 442–454.

Tsutsumi, S., Beebe, K., and Neckers, L. (2009). Impact of heat-shock protein 90 on cancer metastasis. Future Oncol. *5*, 679–688.

Usui, T., Ogawa, H., and Petrini, J.H. (2001). A DNA damage response pathway controlled by Tel1 and the Mre11 complex. Mol. Cell *7*, 1255–1266.

Vichalkovski, A., Gresko, E., Hess, D., et al. (2010). PKB/AKT phosphorylation of the transcription factor Twist-1 at Ser42 inhibits p53 activity in response to DNA damage. Oncogene *29*, 3554–3565.

Vuoriluoto, K., Haugen, H., Kiviluoto, S., et al. (2011). Vimentin regulates EMT induction by Slug and oncogenic H-Ras and migration by governing Axl expression in breast cancer. Oncogene *30*, 1436–1448.

Xia, W., Chen, J.S., Zhou, X., et al. (2004). Phosphorylation/cytoplasmic localization of p21Cip1/WAF1 is associated with HER2/neu overexpression and provides a novel combination predictor for poor prognosis in breast cancer patients. Clin. Cancer Res. *10*, 3815–3824.

Yang, Z., Rayala, S., Nguyen, D., et al. (2005). Pak1 phosphorylation of snail, a master regulator of epithelial-to-mesenchyme transition, modulates snail's subcellular localization and functions. Cancer Res. *65*, 3179–3184.

Yang, M.H., Chang, S.Y., Chiou, S.H., et al. (2007). Overexpression of NBS1 induces epithelial–mesenchymal transition and co-expression of NBS1 and Snail predicts metastasis of head and neck cancer. Oncogene *26*, 1459–1467.

Yang, C., Tang, X., Guo, X., et al. (2011). Aurora-B mediated ATM serine 1403 phosphorylation is required for mitotic ATM activation and the spindle checkpoint. Mol. Cell *44*, 597–608.

Yang, C., Wang, H., Xu, Y., et al. (2012). The kinetochore protein Bub1 participates in the DNA damage response. DNA Repair (Amst.) *11*, 185–191.

Yook, J.I., Li, X.Y., Ota, I., et al. (2005). Wnt-dependent regulation of the E-cadherin repressor snail. J. Biol. Chem. *280*, 11740–11748.

Zhou, B.P., Deng, J., Xia, W., et al. (2004). Dual regulation of Snail by GSK-3beta-mediated phosphorylation in control of epithelial–mesenchymal transition. Nat. Cell Biol. *6*, 931–940.